Structural, Chemical and Morphological of Porous Silicon Produced by Electrochemical Etching

Amna A. Salman
Applied Science Department, University of Technology /Baghdad
Fatima I. Sultan
Applied Science Department, University of Technology /Baghdad
Dr. Uday M. Nayef
Applied Science Department. University of Technology /Baghdad
E-mail: unayef@yahoo.com (Head of group)

ABSTRACT

In this paper, the nanocrystalline porous silicon (PS) films is prepared by electrochemical etching of *p*-type silicon wafer with different currents density (15 and 30 mA/cm^2) and etching times on the formation nano-sized pore array with a dimension of around few hundreds nanometric. The films were characterized by the measurement of XRD, FTIR spectroscopy and atomic force microscopy properties. We have estimated crystallites size from X-Ray diffraction about nanoscale for porous silicon and Atomic Force microscopy confirms the nanometric size

Chemical fictionalization during the electrochemical etching show on surface chemical composition of PS. The etching possesses inhomogeneous microstructures that contain *a*-Si clusters (Si$_3$–Si–H) dispersed in amorphous silica matrix and (O-SiO, C-SiO). From the FTIR analyses showed that the Si dangling bonds of the as-prepared PS layer have large amount of Hydrogen to form weak Si–H bonds.

The atomic force microscopy investigation shows the rough silicon surface, with increasing etching process (current density and etching time) porous structure nucleates which leads to an increase in the depth and width (diameter) of surface pits. Consequently, the surface roughness also increases.

Keywords: Nanocrystalline porous silicon; Anodization; XRD; FTIR; AFM

تركيبية وكيميائية وتراكيب السطوح السليكون المسامي المنتج بالتنميش الكهروكيمياوي

الخلاصة

في هذا البحث تم تحضير أغشية السليكون المسامي النانوية بطريقة التنميش الكهروكيميائي لرقائق السليكون من النوع القابل مع كثافة تيارات (15 و 30 ملي امبير/سم^2) لتكوين حفر بأحجام نانوية منظمة بحدود مئات قليلة من الأبعاد النانومترية وازمان تنميش مختلفة وتم تشخيص الأغشية من قياسات حيود الأشعة السينية ومطيافية تحويلات فورير للأشعة تحت الحمراء وخواص مجهر القوى الذري. من حيود الأشعة السينية تم تخمين الحجم البلوري للسليكون المسامي بالمقياس النانو ومجهر القوى الذري يؤكد على ان الحجم بالنانومتر.

كما تم تحديد المجاميع الفعالة الكيميائية خلال التنميش الكهرو كيمياوي تظهر على سطح المركب الكيميائي للسليكون المسامي. عملية التنميش الكهروكيميائي التي تحوي على تراكيب غير متجانسة في السليكون العشوائي مثل عناقيد (Si$_3$-Si-H) وعلى مجموعات (O-SiO, C-SiO) المشتتة في السليكا العشوائية. من تحليلات تحويلات فورير للاشعة تحت الحمراء أظهرت أواصر السليكون المتدلية لطبقة السليكون المسامي كما تم ترسيبها حيث تحوي كمية كبيرة من الهيدروجين على شكل أواصر Si-H الضعيفة.

أظهرت اختبارات مجهر القوى الذري على سطح السيليكون الخشن ، مع زيادة عملية التنميش (كثافة التيار وزمن التنميش) نوى البنية المسامية الذي تؤدي إلى زيادة في عمق وعرض (القطر) من حفر السطح. وبالتالي فإن الزيادة بخشونة السطح أيضا تزداد.

INTRODUCTION

Porous silicon (PS) consists of a network of nanoscale sized silicon wires and voids which formed when crystalline silicon wafers are etched electrochemically in hydrofluoric acid based electrolyte solution under constant anodization conditions [1]. The optical properties of porous silicon (direct gap, low reflectivity, variable refractive index, red photoluminescence, randomized morphological structure and possibility of band gap engineering) make this material to be a good candidate for photovoltaic applications. [2,3]. Such structures consist of silicon particles in several nanometer size separated by voids. Hence, porous silicon layers are regarded as nanomaterials which can be obtained by the electrochemical etching of silicon wafer. Porous silicon structures has good mechanical robustness, chemical stability and compatibility with existing silicon technology therefore has a wide area of potential applications such as waveguides, 1D photonic crystals, chemical sensors, biological sensors, photovoltaic devices etc. [4]. PS can be a bioactive, a

856

bioinert or a resorbable material, depending on the morphological, chemical and electrical characteristics of the surface layer and those of the biological environment in which it is inserted [5]. This discovery added more interest in the modification of silicon surfaces via formation of Si-C and Si-O-E (E = H, C, N) bonds on silicon surfaces. The most common way for chemical bonding of organic reagents to Si surface is the hydrosilylation of silicon-hydride terminated surfaces [6].

Formation of porous silicon under all possible process conditions, this is partly due to the large number of independent process parameters (etching current, electrolyte composition, wafer doping, duration, illumination, cell construction) [7]. In practice, current density is more accurate in controlling of porosity and reproducibility of the porous layer [8]. HF concentration and the current density usually are in the range of 15-40 wt.% and 1-100 mA/cm^2, respectively [9].

The main objective of this paper is to study the effect of the etching conditions (etching time and current density) on surface changes in silicon (111) is to contribute to the characterization of structural and morphological for PS surface is made by means of XRD and AFM technique respectively. In addition to the characterization of the evolution of the chemical species in the PS surface is made by means of FTIR technique.

EXPERIMENTAL PROCEDURE

Samples used in this study are boron doped crystalline silicon (c-Si) wafers (thickness 508±15μm and resistivity 1.5-4 Ω.cm) grown by Czochralski (CZ) method in (111) orientations. Initially these crystals are characterized by XRD-6000 SHIMADZU Japan, FTIR IRAffinity-1 Fourier Transform Infrared Spectrophotometer SHIMADZU and AFM the atomic force micrographs were taken for porous silicon by AA3000 Scanning Probe Microscope Angstrom Advanced Inc.

The porous samples were then prepared by electrochemical anodic dissolution of doped silicon in 40% hydrofluoric acid and ethanol with gold electrode as cathode. The electrolyte was prepared by mixing HF (40%) and ethanol in 1:2 ratios. The wafer and the solution were placed in a Teflon cell as shown in Fig. 1. The porous layers on the surface of these samples were prepared at current densities of 15 mA/cm^2 and 30 mA/cm^2 with etching times of 10, 30 and 60 min.

857

RESULTS AND DISCUSSION

a. Structural Properties

One important property of porous silicon is that its skeleton maintains the structure of silicon crystalline after anodization, as shown by X-ray topography studies. The X-ray beam is diffracted at specific angular positions with respect to the incident beam depending on the phases of the sample. When crystal size is reduced toward nanometric scale, then a broadening of diffraction peaks is observed and the width of the peak is directly correlated to the size of the nanocrystalline domains [10]

It is well known that crystallites size can be estimated from diffraction pattern analysis by measuring the full width at half maximum (FWHM) measurement and applying the Scherrer equation:

$$L = \frac{K\lambda}{B cos\theta_B} \dots \dots \dots \text{(1)}$$

Where *B* is the FWHM in radians, *K* is the Scherrer constant ($1 > K > 0.89$), λ is the wavelength in nanometers, θ_B in radians is the diffraction angle and *L* the mean crystallite size [11].

Fig. (2) and Fig. (3), shows typical diffraction pattern of PS sample fabricated at etching current density of 15 and 30 mA/cm^2 respectively at different etching times

The crystallites size obtained for crystalline and porous silicon samples are shown in Table (1), when estimated by the Scherrer equation, a significant crystallites size decrease trend can be clearly noted on increasing etching times and current density, in the case of porous samples, nanometric dimensions are achieved in considerably shorter times.

The porous structure and the decrease of the Si size because a broadening of the Si plane (111) peaks.

The effect of nanocrystallite size is interpreted as widening of bandgap of the PS layer due to the quantum confinement phenomenon. One of the most important methods to determine energy bandgap is by using X-ray diffraction and by photoluminescence spectra [12] .

The energy bandgap of PS layer can be calculated dependence on the size of crystals as follows [13]:

858

$$E_g^* = E_g + \frac{88.34}{L^{1.37}} \dots \dots \dots (2)$$

Where E_g^* (eV) is the energy bandgap of PS layer, E_g (eV) is the energy bandgap of bulk silicon and L (Å) is nanocrystallite size.

From the table (1) we shown in different etching process will lead to form PS layer with higher energy bandgap and smaller silicon nanosizes within the PS layer, which is bigger than that for crystalline silicon substrate 1.12 eV (indirect, 300K) [14].

b. Chemical Composition of PS Layer

Surface chemical composition of PS is best probed with Fourier Transform Infrared (FTIR) spectroscopy. FTIR signal in PS is larger and easier to measure than in bulk Si due to much larger specific area.

The pore surface includes a high density of dangling bonds of Si for original impurities such as hydrogen and fluorine, which are residuals from the electrolyte. Additionally, if the manufactured PS layer is stored in ambient air for a few hours, the surface oxidizes spontaneously.

The FTIR spectra of the p-type porous silicon are shown in curve (a) and (b), in Fig. 4 show the FTIR spectra measured from samples of: (a) at current density 15 mA/cm^2 and etching time 30 min. and (b) current density 30 mA/cm^2 and etching time 30 min.

The peaks at around 439.77 cm^{-1} and 1064.71 cm^{-1} are from Si–O–Si stretching modes [15], which are dependent on the oxidation degree of porous silicon. The transmittance peak at 624.94 cm^{-1} Si-H bending in (Si$_3$SiH), 871.82 cm^{-1} Si-H$_2$ wagging mode and 910.4 cm^{-1} Si-H$_2$ scissor mode [16,17]. The transmittance peak at 1458.18 cm^{-1} C-H$_3$ asymmetric deformed and 1705.07 cm^{-1} related to C-O Furthermore, 2090.84 cm^{-1} and 2924.09 cm^{-1} are, respectively, related to Si–H stretch (Si$_3$-SiH) and C-H stretch (CH$_2$) [18,19].

Chemical bonds and their IR resonance positions detected in PS are shown in Table (2).

c. Morphological Properties

The surface morphology of the oxidized PS layers was investigated using Atomic force microscope (AFM) studies focus entirely on the nanoscale characterization of PS films.

When etching time increases a part of pores coagulate to larger structures. Fig. 5 and Fig. 6, shows the 2D and 3D AFM image of porous silicon in which the irregular and randomly distributed nanocrystalline silicon pillars and voids over the entire surface can be seen. The prepared porous silicon layer shows the surface roughness and pyramid like hillocks surface.

Pore morphology when current flows in the electrochemical cell, the dissociation reaction localizes on a particular side of a silicon surface, thus initiating the etching of an array of pores in the silicon wafer. At low current density, a highly branched, randomly directed and highly inter-connected meshwork of pores was obtained. However, increasing in current density orders the small pores [20].

Fig. 5 and Fig. 6 show with increasing potential porous structure nucleates which leads to an increase in the depth and width (diameter) of surface pits. Consequently, the surface roughness also increases. Changes in the roughness and the height of the surfaces mean were revealed. Table (3) gives the roughness average and root mean square.

CONCLUSIONS

Porous silicon layers are prepared by electrochemical etching for different current densities and etching times. The samples are then characterized the nanocrystalline porous silicon layer to study its structural, chemical and morphological properties.

From the XRD properties we have shown the porous structure and the decrease of the Si nano-sized because a broadening of the Si peaks.

In porous silicon, as-prepared samples, oxygen is normally absent, the dominant bonds being Si-H groups (x = 1, 2 or 3).

The atomic force microscopy investigation shows the rough silicon surface which can be regarded as a condensation point for small skeleton clusters which plays an important role for the characterized the nanocrystalline porous silicon. However, the isolated silicon pillars with steeper sidewalls confirm the achieving of quantum confinement effect. The changes of the silicon surface morphology due to the etching in electrolytes with slightly different anodic dissolution.

REFERENCES

[1] Šalucha, D. K. and A. J. Marcinkevičius, "Investigation of Porous Silicon Layers as Passivation Coatings for High Voltage Silicon Devices", ISSN 1392-1215 Electronics and Electrical Engineering, No. 7(79) 41-44 (2007).

[2] Nichiporuk, O. A. Kaminski, M. Lemiti, A. Fave, S. Litvinenko, V. Skryshevsky, "Passivation of the surface of rear contact solar cells by porous silicon", Thin Solid Films 511-512, 248-251 (2006)

[3] Bratkowski, A. A. Korcala, Z. £ukasiak, P. Borowski, and W. Bala, "Novel Gas Sensors Based on Porous Silicon measured by Photovoltage, Photoluminescence, and admittance Spectroscopy", Opto-Electron. Rev., 13, no. 1, 35-38 (2005).

[4] Dubey, R. S. and D. K. Gautam, "Synthesis and Characterization of Nanocrystalline Porous Silicon Layer for Solar Cells Applications", Journal of Optoelectronic and Biomedical Materials Volume 1, Issue 1, 8-14, March (2009).

[5] Ioanid, A. M. Dieaconu, S. Antohe, "A Semiempirical Potential Model for H-Terminated Functionalized Surface of Porous Silicon", Digest Journal of Nanomaterials and Biostructures Vol. 5, No 4, 947-957 October-December (2010).

[6] Gun'ko, Y. K. T. S. Perova, S. Balakrishnan, D. A. Potapova, R. A. Moore and E. V. Astrovac "Spectroscopic characterization of chemically modified porous silicon", Proceedings of SPIE Vol. 4876, 788-795 (2003).

[7] Evangelos A. Angelopoulos, Saleh Ferwana, Martin Zimmermann, Elisabeth Penteker, and Joachim N. Burghartz, "Porous Silicon for Micro- and Optoelectronic Applications: Fabrication Technology and Post-Processing Steps".

[8] Salem, M. S. M. J. Sailor, F. A. Harraz, T. Sakka, and Y. H. Ogata, "Electrochemical Stabilization of Porous Silicon Multilayers for Sensing Various Chemical Compounds", J. of Appl. Phys. 100, 083520 (2006).

[9] Jakubowicz, J. "Morphology of Silicon (111) During Electrochemical Etching in NH_4F Electrolytes", Advances in Materials Science, Vol. 5, No. 2 (7), June (2005).

[10] Lorusso, A. V. Nassisi, G. Congedo, N. Lovergine, L. Velardi, P. Prete, "Pulsed plasma ion source to create Si nanocrystals in SiO_2 substrates", Applied Surface Science, 255, 5401-5404 (2009).

[11] Luigi Russo, Francesco Colangelo, Raffaele Cioffi, Ilaria Rea and Luca De Stefano, "A Mechanochemical Approach to Porous Silicon Nanoparticles Fabrication", Materials 4, 1023-1033 (2011).

[12] Anyamesem, B. "The Formation of Silicon Nanoparticles on Silicon-on Insulator Substrate by Thermal Anneal", Thesis University of Texas, (2007).

[13] Timokhov, D. F. and F. P. Timokhov, "Determination of Structure Parameters of Porous Silicon by the Photoelectric Method", J. Phys. Studies 8 (2), 173-177 (2004).

[14] Sze, S. M. and K. K. Ng, "Physics of Semiconductor Devices", 3[ed] Copyright © (2007) John Wiley & Sons, Inc.

[15] Yue Zhao, Deren Yang, Dongsheng Li, Minghua Jiang, "Annealing and amorphous silicon passivation of porous silicon with blue light emission", Applied Surface Science 252, 1065–1069 (2005).

[16] Bisis, S. Ossicini and L. Pavesi, "porous silicon: a quantum sponge structure for silicon based optoelectronics", Surface science reports 264, (2000).

[17] Arce, R.D. R.R. Koropecki, G. Olmos, A.M. Gennaro, J.A. Schmidt, "Photoinduced Phenomena in Nanostructured Porous Silicon", Thin Solid Films 510, 169-174 (2006).

[18] PAP, A. E. "Investigation of Pristine and Oxidized Porous Silicon", Thesis University of Oulu, (2005).

[19] Dimova - Malinovska, D. "Application of Stain Etched Porous Silicon in c-Si Solar Cells", Optoelectronics Review 8(4), 353-355 (2000).

[20] Patel, A. K. "Use of Electrochemically Machined Porous Silicon to Trap Protein Molecule", J. of Appl. Sci., Engineering and Technology 2(3): 208-215, (2010).

Table (1): Crystallites size obtained by means of Scherrer equation and energy gap of PS layer which prepared under different etching process.

Current density (mA/cm^2)	Etching time (min)	Crystallites size (nm)	Energy Bandgap (eV)
15	30	4.262	1.637
30	10	4.390	1.616
	30	3.897	1.704
	60	3.847	1.715

Table (2): Wavenumber positions and attributions of the transmittance peaks observed in several PS samples by Fourier transform infrared absorption FTIR measurements.

Peak position (cm^{-1})	Attribution
439.77	Si-O stretching in Si-O-Si
624.94	Si-H bending in (Si_3-SiH)
871.82	$Si-H_2$ wagging
910.4	$Si-H_2$ scissor
1064.71	Si-O stretching in O-SiO and C-SiO
1458.18	$C-H_3$ asymmetric deformed
1705.07	C-O
2090.84	Si-H stretch. (Si_3-SiH)
2924.09	C-H stretch. (CH_2)

Table (3): The calculated morphology characteristics of PS samples prepared with different etching process

Current density (mA/cm^2)	Etching Time (min)	Roughness Ave. (nm)	RMS (nm)
15	10	5.56	12.2
	30	13.6	18.9
	60	26	33.5
30	10	0.7	2.2
	30	3.06	4.85
	60	24.1	30.8
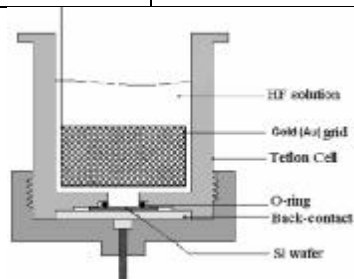
Figure (1) Schematic diagram of the porous silicon anodization
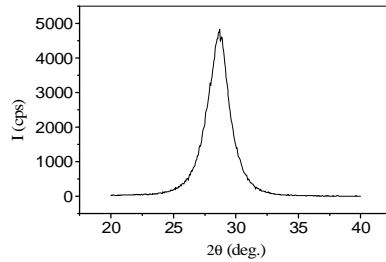
Figure (2) Shows X-ray diffraction of porous silicon prepared by current density 15 mA/cm^2 and etching time etching time 30 min

(a)

(b)

(c)
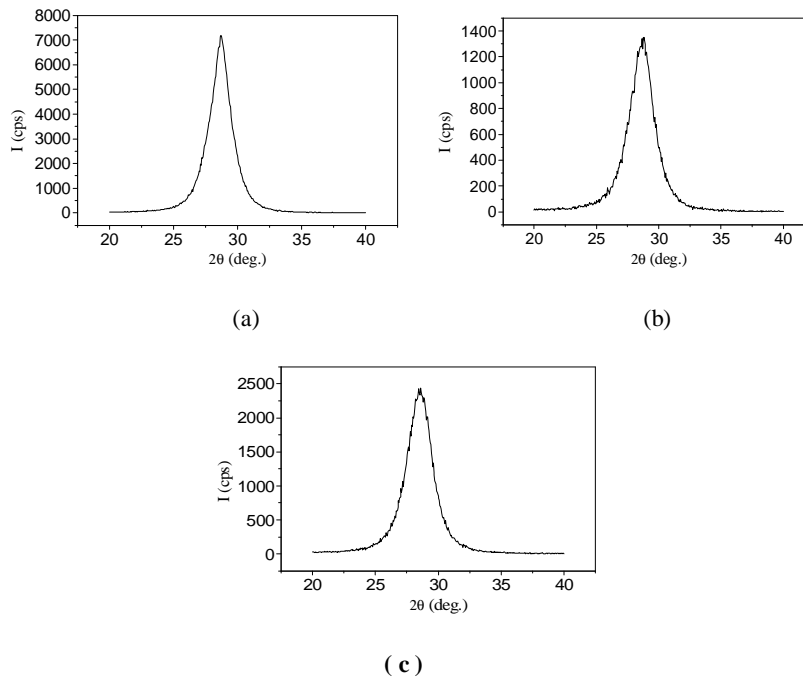
Figure (3) Shows X-ray diffraction of porous silicon prepared by current density 30 mA/cm^2 and different etching time etching time a) 10 b) 30 c) 60 min
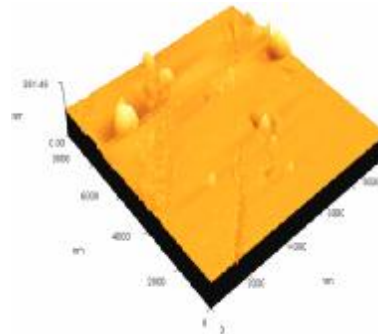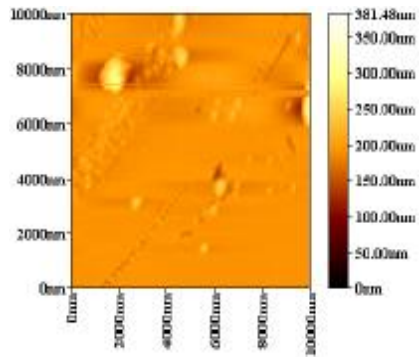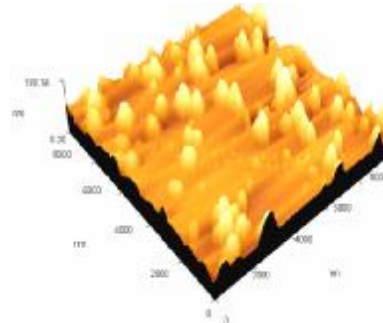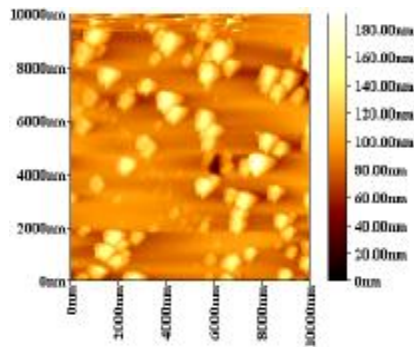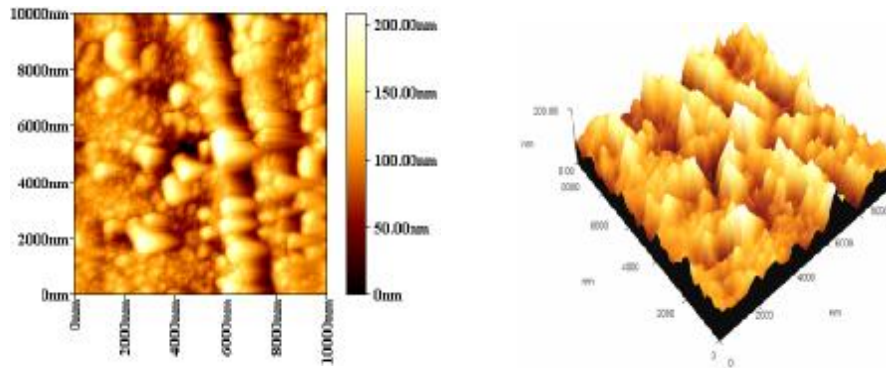
864
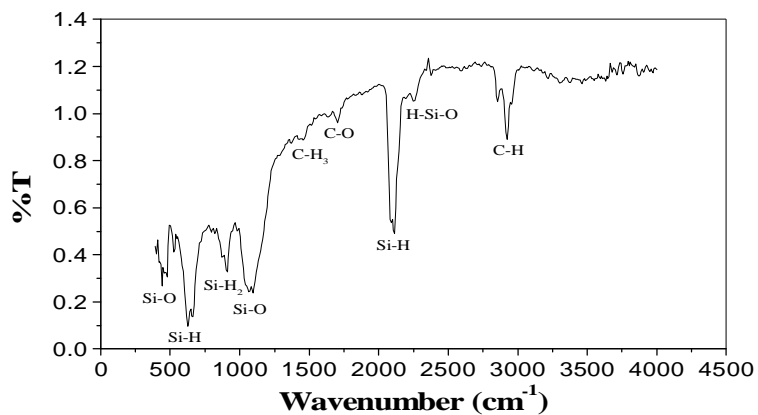
(a)
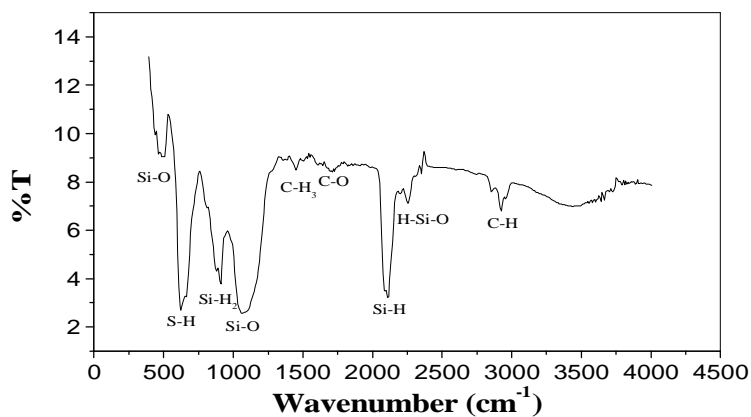
(b)

Figure (4) IR transmittance spectrum of a PS layer
(a) 15 mA/cm^2 (b) 30 mA/cm^2 at etching time 30 min

865

(**a**)

(**b**)

866
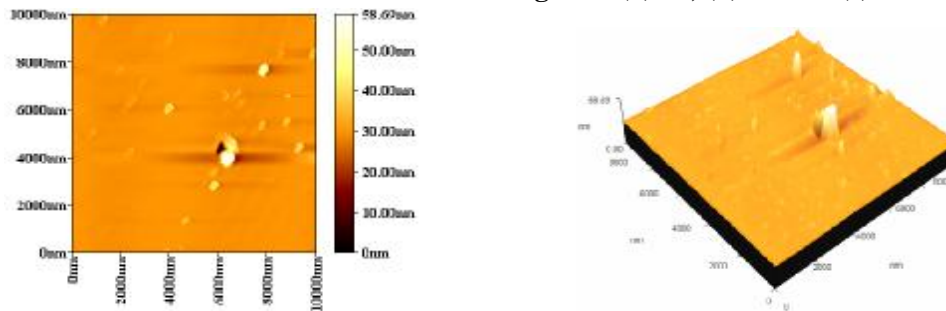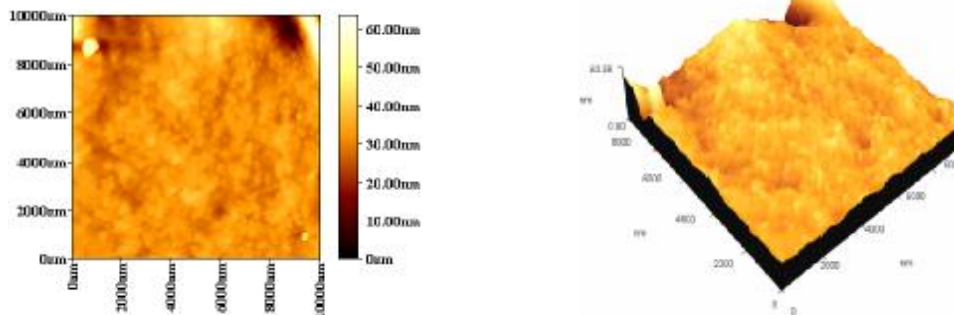
(c)

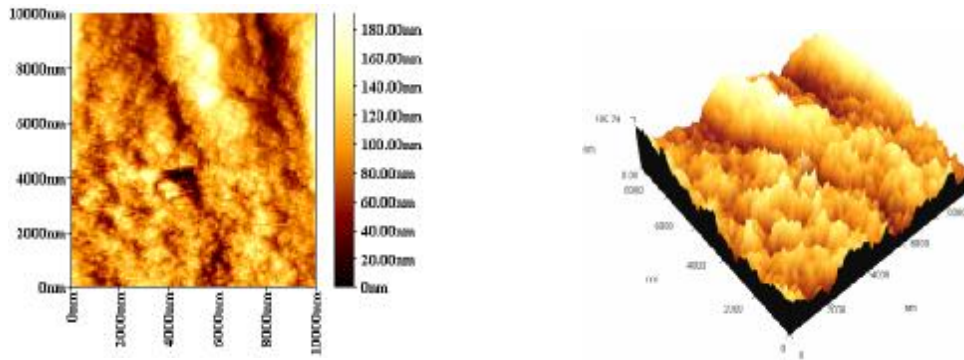**Figure (5) 2D and 3D AFM image of porous silicon monolayer prepared at
J=15 mA/cm^2 etched under different etching time (a) 10, (b) 30 and (c) 60 min.**

(a)

(b)

867

(c)

Figure (6) 2D and 3D AFM image of porous silicon monolayer prepared at J=30 mA/cm^2 etched under different etching time (a) 10, (b) 30 and (c) 60 min.

868